JOURNAL OF CATALYSIS 123, 364–374 (1990)

Reduction of Ni^{2+} Cations in Y Zeolites

I. Effect of Sample Pretreatment

BRENDAN COUGHLAN AND MARK A. KEANE[1]

Physical Chemistry Laboratories, University College, Galway, Ireland

Received August 10, 1989; revised October 11, 1989

A range of NiNa–Y and NiK–Y zeolites was prepared by ion exchange. The location of Ni^{2+} cations within the zeolite framework was monitored after various stages of thermal treatment and the reduction process of the transition metal ion in a flowing hydrogen atmosphere was investigated and correlated with such factors as the hydrogen flow rate, reduction time, reduction temperature, sample precalcination, and NH_3 pretreatment. Cation location was probed by means of Cs^+ back exchange and confirmed by the observation of the IR spectra of CO adsorbed on the activated zeolites. Iodometric titrations and Na^+ back-exchange techniques were used to measure the levels of Ni^{2+} reduction. The data generated reveal how the interrelated Ni^{2+} ion location and the nature of the charge-balancing alkali metal co-cation serve to influence the level of Ni^{2+} reduction.

INTRODUCTION

The most common procedure for incorporating metals into zeolites involves the introduction of the hydrated metal ion by the process of ion exchange followed by reduction of the cation in a reducing atmosphere. The factors affecting the reduction process have been the subject of multilateral investigations. A scan through the literature reveals the complex nature of the system; reducibility has been found to depend strongly on zeolite structure, pretreatment conditions, and the initial cation location. According to the nature of the cation and the type of zeolite, various mechanisms for the reduction process have been proposed. Delafosse (*1*) has classified the main factors which govern the reducibility of transition metal cations as: (a) those which depend on the nature of the cation; (b) those which depend on the zeolite type, symmetry, and chemical composition; (c) those which depend on the local environment of the cation; (d) those which are due to the nature of the reducing agents.

The reduction of exchanged nickel cations in zeolites has been extensively studied due to the catalytic applications inherent in the system. Molecular hydrogen is the most frequently used agent to reduce divalent nickel cations in a zeolite framework (*2–4*). It is also possible to reduce nickel ions by other reagents such as NH_3 (*5*), CO (*6*), and atomic hydrogen at very low temperatures. Rabo (*7*), in one of the earliest studies, found that Ni^{2+} ions supported on Y zeolite were reduced to the metallic state at temperatures above 473 K; Penchev *et al.* (*8*), in contrast, reported that reduction of divalent nickel with hydrogen begins at 523–573 K. The data on nickel-exchanged zeolite Y are complicated by incomplete exchange and the presence of water, even after dehydration at elevated temperatures (*9*). Notwithstanding this, the degree of nickel reduction has been reported to increase with reduction temperature (*10*). In the majority of studies, the nickel-supported zeolite samples were evacuated or dehydrated in inert media prior to reduction. It has been shown (*10–*

[1] To whom correspondence should be addressed at Chemistry Dept., University of Glasgow, Glasgow G12 8QQ, United Kingdom.

0021-9517/90 $3.00

13) that dehydration before reduction diminishes the extent of reduction. This is explained on the basis of Ni^{2+} migration to S_I positions (in the hexagonal prisms) where the cations are stabilized in an octahedral environment and are less susceptible to reduction. In any case, reduction of Ni^{2+} in faujasite is usually incomplete (*14–16*). Lawson and Rase (*17*) observed that reduction at low temperatures for long periods of time ensured that most of the divalent nickel was reduced whereas Derouane *et al.* (*18*) obtained 100% reduction of $Ni_{18}Na$–Y at 873 K, the sample having been previously outgassed at 373 K. At high temperatures (>600K) NH_3 has proved to be a more effective reducing agent than molecular hydrogen (*5*). At these elevated temperatures NH_3 decomposes to form active hydrogen which can reduce Ni^{2+} ions in the more "hidden" hexagonal prism sites; similarly, workers using atomic hydrogen have been able to obtain very high levels of reduction (*19*).

As a prerequisite to understanding the process of cation reduction in zeolites, the positions of the cations in the framework must be known. There are certain preferred locations and the cations confer individual properties on the surface of the zeolite cavities dependent on their charge, electronic structure, and ligancy. The accessibility of nickel ions for reduction depends on the initial cation location and the residual water content. The local environment of the Ni^{2+} cation must therefore be taken into account. The standpoint as regards the relative stability of Ni^{2+} ions in "hidden" and "open" sites is ambiguous with some workers reporting that Ni^{2+} ions at S_I sites are more easily reduced (*5, 20–22*). Gallezot *et al.* (*23*) found that, on hydrogen reduction at 633 K, only the Ni^{2+} ions from S_{II} sites in the sodalite cages are reduced; reduction of Ni^{2+} ions in the hexagonal prisms occurs at much higher temperatures. Nevertheless, considerable experimental data on NiNa–Y point to nickel ions in supercage positions being preferentially reduced at lower temperatures; only under extreme conditions are Ni^{2+} ions in the hexagonal prisms reduced (*10, 12, 24*).

This paper is the first of a series devoted to unravelling some of the anomalies surrounding the phenomenon of Ni^{2+} reduction in zeolites. It can be argued that this lack of consistancy stems from the difficulty in isolating the variables which may affect the reduction process. In addition, all of the studies to date have concerned the exchanged parent Na–Y zeolite with no reported data on nickel exchanged Li, K, Rb, or Cs forms. Unfortunately, because of the variety of experimental conditions used, particularly with regard to sample pretreatment, one may only, at best, make tentative, qualitative comparisons with the reported data on degree of cation reduction. It was therefore thought prudent to investigate the effects of sample pretreatment as a prelude to a study of the respective roles of nickel loading and sample acidity on the reduction process.

METHODS

The starting or parent zeolite was Linde molecular sieve LSZ-52 [formula: $Na_{58}(AlO_2)_{58}(SiO_2)_{134}(H_2O)_{260}$]. KY was prepared by refluxing 250 g of Na–Y with 400 cm^3 of 1 *M* KNO_3 for 24 h, after which the zeolite was vacuum filtered and thoroughly washed with hot deionized water to remove the occluded salt. The zeolite was then oven dried at 373 K for a further 24 h; this heat treatment provided the necessary energy of activation to accomplish a redistribution of the exchanged ions. The resultant KNa–Y samples were exchanged an additional nine times and stored over saturated NH_4Cl solutions. NiNa–Y and NiK–Y samples were prepared by taking 100 g of Na–Y or K–Y and refluxing with a 400 cm^3 $Ni(NO_3)_2$ solution for 24 h. The pH of the Na–Y zeolite/deionized water suspension was 9.5. It has been reported that many transition metal salt solutions are sufficiently acidic to cause structural breakdown (*25*). In this study, dilute nickel ni-

trate solutions (<0.1 *M*) were employed in which the pH (as monitored by a pH meter) of the nitrate/zeolite suspension was in the range 6–7.5. Under these conditions, a single exchange cycle resulted in a maximum exchange of ca. 7 Ni^{2+}/UC, i.e., seven nickel cations per unit cell. In preparing samples with loadings greater than ca. 7 Ni^{2+}/UC, repeated exchange was necessary. Atomic absorption (Ni^{2+} concentration) and flame emission (Na^+ and K^+ concentrations) techniques, using a Perkin–Elmer 360 atomic absorption spectrophotometer, were employed to determine the cation content. Samples were prepared for analysis by treating 0.2 g of the hydrated zeolites with 20 cm^3 conc. HCl and stirring at room temperature for 16 h. The resultant suspension was then filtered and made up to 250 cm^3 with deionized water. Measurements were made in the 0–5 ppm range by performing the appropriate dilutions. The standards employed were prepared from stock solutions supplied by BDH Chemicals Ltd. From the measured ion concentrations, the precise mass of the zeolite sample, and the number of unit cells per gram of parent zeolite (3.5×10^{19} for Na–Y and 3.3×10^{19} for K–Y), the number of nickel cations per unit cell were determined. Thermal analyses were also conducted on all the prepared samples using a Perkin–Elmer thermobalance operating in the TG mode to measure water loss as a function of temperature.

The percentage reduction of Ni^{2+} ions, supported on both Na–Y and K–Y carriers in flowing hydrogen, was obtained using iodometric and Na^+ back-exchange techniques. In both cases, 3 g of hydrated sample, in pellet form (1.18–1.70 mm diameter), were reduced in a fixed-bed catalytic reactor (*26*), normally in a 120 cm^3 min^{-1} stream of hydrogen at 723 K for 18 h. However, these conditions were also varied, the effects of which will be outlined in the discussion section. The zeolite pellets were supported between two layers of glass beads. The thermocouple used to monitor the reduction temperature was embedded in the zeolite layer. The heating system (*26*) normally employed only allowed for a variable rate of heating of the samples. In the experiments where a fixed rate of heating was desired, a temperature programmer/controller (Cambridge Process Controls Model 702) was used. The model 702 automatic controller is a combined sequence/ramp programmer and temperature control system. The microprocessor system in the unit allows fully automatic operation of the furnace through the complete operating cycle to a time and temperature sequence program stored in the unit's memory. After reduction, the samples were stored over saturated NH_4Cl and the water content was determined before degree of reduction measurements were conducted.

Iodometric Titration

One gram of hydrated reduced sample, in powder form, was refluxed at 373 K for 16 h with 20 cm^3 of 0.1 *M* $K_2Cr_2O_7$, the suspension was filtered, and the filtrate was made up to 250 cm^3; 50 cm^3 of this solution was then transferred to a 500-cm^3 volumetric flask with 100 cm^3 of recently boiled deionized water, 6 cm^3 conc. HCl, 2 g $NaHCO_3$, and 3 g KI. The resulting solution was left to develop in the dark for 15 min after which the volume was made up to 500 cm^3 with deionized water; 50 cm^3 of this solution was then titrated against standardized 0.01 *M* $Na_2S_2O_3$ using starch as indicator. The unreduced sample was also carried through the procedure as a blank and the amount of nickel metal present was determined from the difference in reading between the blank and the sample.

Na^+ Back Exchange

One hundred milligrams of the hydrated reduced zeolite, in powder form, was immersed in 50 cm^3 of 1 *M* $NaNO_3$ and the resultant suspension refluxed for 24 h. In this process, the Na^+ ions will only be exchanged with the unreduced Ni^{2+} cations. On filtering the solution, the filtrate was

made up to 100 cm^3 and analyzed for Ni^{2+} ions by atomic absorption in the 0- to 5-ppm range. The procedure was also repeated using the unreduced zeolite as a blank. The degree of reduction (α) is then given by

$$\frac{\text{ppm } Ni^{2+} \text{ in unreduced sample} - \text{ppm } Ni^{2+} \text{ in reduced sample}}{\text{ppm } Ni^{2+} \text{ in unreduced sample}}.$$

The reduction data obtained from both techniques were in close agreement. The values quoted in this paper are those generated by iodometric titration.

The location of Ni^{2+} ions in the dehydrated zeolite framework was studied using a Cs^+ back-exchange technique. In this case, the zeolite bed (*26*) was heated in a stream of nitrogen (120 cm^3 min^{-1}) to a final temperature of 723 K which was maintained for 18 h. The rehydrated calcined sample (as a fine powder) was then added to a 2 *M* CsCl solution and the resultant suspension vigorously stirred at room temperature for 16 h. The Cs^+ ions will exchange out any large cage Ni^{2+} ions but because of their size are unable to enter the sodalite units or hexagonal prisms (*27*). The number of Ni^{2+} cations remaining in the small cages was then determined by atomic absorption.

IR spectra were obtained of CO adsorbed on a range of calcined nickel zeolites. The spectra were recorded using a special portable vacuum cell (*26*). The zeolite samples were in the form of self-supporting disks of surface area 1.3 cm^2 prepared by compressing 10 mg of fine zeolite powder under a pressure of 4 kg cm^{-2} for 5 min using a Beckman 25-ton hydraulic press. The vacuum cell, with the disk inserted, was outgassed ($<1.3 \times 10^{-3}$ N m^{-2}) for 1 h at room temperature. The disk was then heated in a stream of nitrogen (120 cm^3 min^{-1}) to a final temperature of 723 K, which was maintained for a further 18 h. The cell was then kept under vacuum and allowed to cool to room temperature and contacted with 2.66×10^3 N m^{-2} CO. The CO, obtained from Irish Industrial Gases, was dried before use over a bed of activated zeolite 4A. The spectra were recorded in the percentage transmission mode.

RESULTS AND DISCUSSION

(*a*) *Chemical Composition of the Samples*

The chemical compositions of the ion-exchanged samples are given in Table 1. The names of the samples are followed, for example in the case of nickel-exchanged K–Y (NiK–Y), by a figure showing the exchange level of Ni^{2+} as a percentage of the total cation exchange capacity. By and large, the exchange process was stoichiometric. The extent of hydrolysis, as evidenced by the number of protons present in the structure, was slight and occurred only for the lower exchanged samples. On calcination at 723 K, the nickel-exchanged zeolites exhibited ill-defined infrared bands in the hydroxyl stretching region.

(*b*) *Ni^{2+} Cation Location*

By employing a Cs^+ back-exchange technique, the location of Ni^{2+} ions in the zeolite lattice during different calcination steps and hence the effect of sample pretreatment on ion location and reduction was probed. The structure of zeolite Y and the precise nature of each cation site have been described in detail by Breck (*28*). Interest-

TABLE 1

Chemical Compositions of the Nickel-Exchanged Zeolites

Zeolite sample	$Na^+(K^+)$/UC	Ni^{2+}/UC	H^+/UC	Water content (wt%)
Na–Y	58.00	—	—	25.08
NiNa–Y-22.76	44.00	6.60	0.80	26.61
NiNa–Y-35.73	36.02	10.42	1.14	27.63
NiNa–Y-63.10	22.32	18.30	—	29.48
K–Y	58.00	—	—	22.41
NiK–Y-23.52	44.18	6.82	0.18	23.54
NiK–Y-35.62	36.87	10.33	0.47	24.81
NiK–Y-49.07	29.77	14.23	—	26.37
NiK–Y-54.48	26.22	15.80	0.18	26.91
NiK–Y-62.52	22.30	18.13	—	27.60
NiK–Y-73.79	16.30	21.40	—	28.04
NiK–Y-81.97	13.13	23.77	—	28.43
NiK–Y-86.62	8.36	25.12	—	29.34
Ni–Y	—	29.00	—	30.16

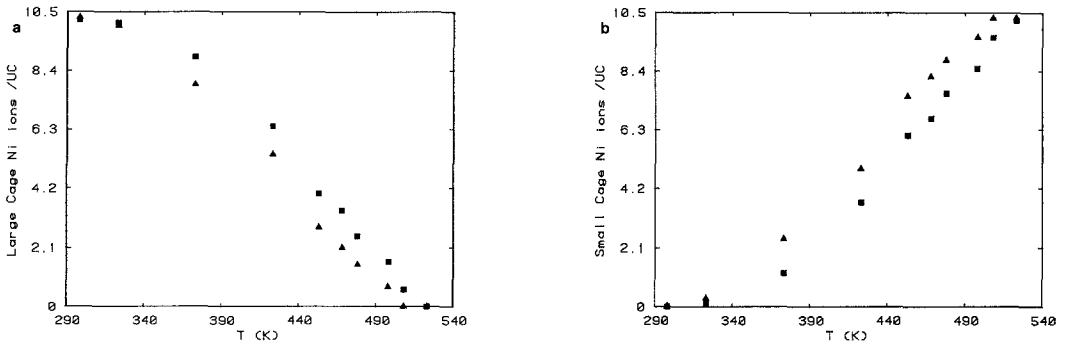

FIG. 1. Variation in the number of (a) large cage and (b) small cage Ni^{2+} cations supported on NiNa–Y-35.73 (▲) and NiK–Y-35.62 (■) with increasing temperature (calcined in a N_2 flow of 120 cm^3 min^{-1} for 18 h).

ingly, on treating the fully exchanged Na–Y and K–Y samples, the K^+ ions exhibited a higher occupancy (26.6 K^+/UC) of the small cage sites than the Na^+ ions (21.9 Na^+/UC). This variation in occupancy must be considered as a parameter in minimizing the free energy of the system. The larger K^+ ions, therefore, in locating preferentially at the hidden, well-shielded S_I and $S_{I'}$ sites lower the overall potential energy of the zeolite lattice to a greater extent than is the case for Na–Y. The value of 26.6 small cage K^+ ions implies an occupancy of 31.4 K^+ ions in the large cages. This value closely agrees with the electrostatic model proposed by Smith (*29*). The consequence of such a variation in the site preference of the alkali metal cations on the location of the Ni^{2+} ions exchanged into Na–Y and K–Y was considered. Figures 1 and 2 follow the concentration of small cage and large cage ions as a function of temperature for two samples of NiNa–Y and NiK–Y of similar nickel loading. The maximum number of Ni^{2+} cations accommodated in the small cages is ca. 12, which is somewhat lower than the values determined using crystallographic methods (*24, 30, 31*). This limiting value of ca. 12 Ni^{2+}/UC is independent of the alkali metal co-cation. For both NiNa–Y and NiK–Y systems, the Ni^{2+} cations originally located in the supercages migrate to the small cages at elevated temperatures. This is consistent with the

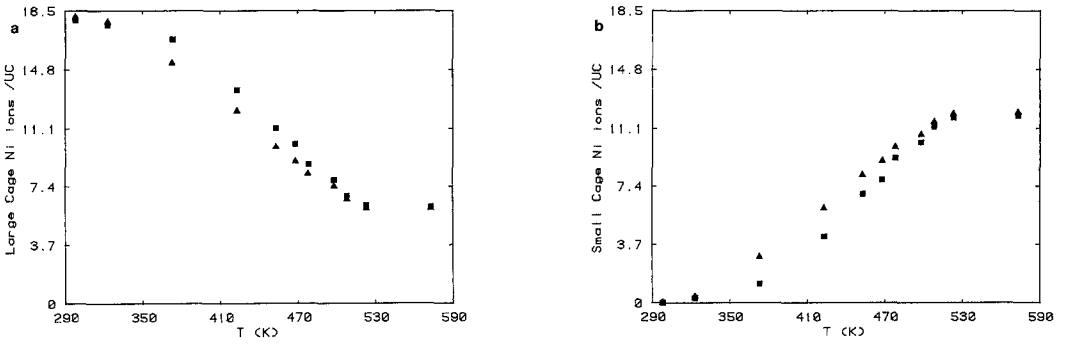

FIG. 2. Variation in the number of (a) large cage and (b) small cage Ni^{2+} cations supported on NiNa–Y-63.10 (▲) and NiK–Y-62.52 (■) with increasing temperature (calcined in a N_2 flow of 120 cm^3 min^{-1} for 18 h).

well-established argument that once most or all of the hydration sheath has been stripped, the nickel cation will diffuse through the six-membered ring and occupy the small cage sites where it can have an octahedral coordination with the framework oxygens, i.e., at S_I sites. The occupation of the small cage sites was also found to be independent of the rate of heating of the samples (varied from 25 to 1000 K h^{-1}) in nitrogen. However, saturation of the small cage sites in K–Y occurs at a higher temperature (ca. 523 K) than that in Na–Y (ca. 493 K). This is presumably due to a greater competition between the Ni^{2+} and K^+ ions for the hidden sites. The rehydrated calcined samples were also contacted with a saturated solution of $NaNO_3$ in order to elute the Ni^{2+} cations. The measured sodium exchange capacities are given in Table 2. The values remain virtually constant for nickel loadings greater than ca. 10 Ni^{2+}/UC. On calcining these samples, the divalent nickel ions driven into the small cages therefore remain effectively "locked" at the S_I sites upon rehydration.

A second physicochemico approach was adopted to study the distribution of Ni^{2+} ions in Na–Y and K–Y, i.e., the observation of the IR spectra of CO adsorption on activated zeolites. Carbon monoxide is a particularly attractive choice for such work. The CO molecule is small enough to enter the supercages of zeolite Y, but too large to enter the sodalite units or hexagonal prisms. The molecule has an asymmetric charge distribution and is easily polarized; it is therefore sensitive to the strong electrostatic field surrounding the exchanged cations. CO adsorption on dehydrated nickel-exchanged samples yielded a spectrum in the ν_{CO} range which included four bands at 2216, 2200, 2170, and 2140 cm^{-1}, in good agreement with the literature values (*32, 33*). The latter two bands were also observed for CO adsorbed on Na–Y and K–Y and may be ascribed to CO physically adsorbed on the zeolite framework. The peaks at 2216 and 2200 cm^{-1} must be due to CO adsorbed on active nickel ions. On studying the adsorption process for a number of nickel-exchanged zeolites, the spectra in the range 2300–2190 cm^{-1} were featureless up to a level of exchange greater than ca. 10 Ni^{2+}/UC. At higher nickel loadings, the intensity of the 2216- and 2200-cm^{-1} bands increased with the number of nickel ions per unit cell (Fig. 3).

TABLE 2

Room Temperature Sodium Exchange Capacities of a Range of Nickel-Exchanged Y Zeolites Calcined at 723 K

Zeolite sample	Ni^{2+}/UC	Na^+ exchange capacity (%)
NiNa–Y-22.76	6.60	76.90
NiNa–Y-35.73	10.42	66.10
NiNa–Y-63.10	18.30	64.90
NiK–Y-23.52	6.82	76.36
NiK–Y-35.62	10.33	65.16
NiK–Y-62.52	18.13	64.48
NiK–Y-81.97	23.77	64.11

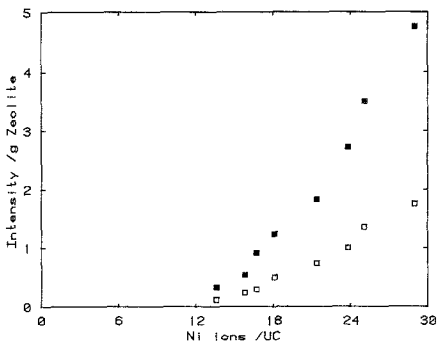

FIG. 3. Plot of the intensities of the 2216 (■) and 2200 (□) cm^{-1} IR bands due to the adsorption of CO on a range of calcined (in a 120 cm^3 min^{-1} flow of N_2 at 723 K for 18 h) NiK–Y samples as a function of nickel loading.

(c) *The Role of Reduction Temperature*

The variation in degree of reduction with temperature for two NiK–Y samples of different nickel loading is illustrated in Fig. 4. The level of Ni^{2+} reduction increases pro-

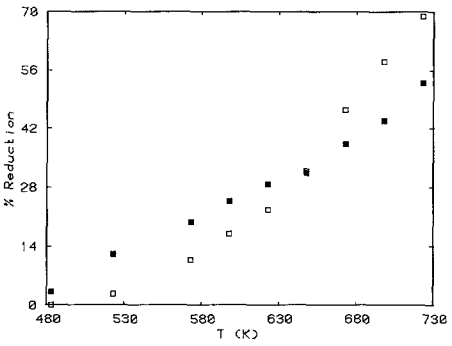

FIG. 4. Effect of reduction temperature (at a H_2 flow rate of 120 cm^3 min^{-1} for 18 h) on the degree of reduction of Ni^{2+} ions supported on NiK–Y-23.52 (□) and NiK–Y-81.97 (■).

gressively with reduction temperature; the extent of reduction is notably greater at lower temperatures for the zeolite sample with the higher metal loading. From the Ni^{2+} cation location study, at temperatures greater than 523 K, all the Ni^{2+} ions in NiK–Y-23.52 (6.82 Ni^{2+}/UC) are located in the small cages whereas ca. 12 Ni^{2+} ions remain in open positions for the NiK–Y-81.97 (23.77 Ni^{2+}/UC) sample. It follows from the degree of reduction data that some cation reduction, more pronounced in the latter case, has taken place below 523 K, i.e., at the temperature where the cation becomes fixed at specific sites. One may therefore infer that reduction of the partially dehydrated Ni^{2+} species has occurred. This is in contrast with the general assumption that complete dehydration is essential before cation reduction commences.

Indeed, the role of cation location in nickel reducibility continues to be a matter of some debate. From the percentage Ni^{2+} reduction versus temperature curves (Fig. 4 and 5), it is apparent that the difference in nickel loading results in different reduction behavior. In the case of the NiK–Y-81.97 (23.77 Ni^{2+}/UC) sample, the extent of reduction increases smoothly with reduction temperature. However, there is a marked increase in Ni^{2+} reduction for NiK–Y-23.52 (6.82 Ni^{2+}/UC) in the temperature range 673–723 K, which is indicative of a greater ease of S_I Ni^{2+} reduction. The fact that such an enhancement in reduction is not observed for the higher loaded sample indicates that the accessible, supercage Ni^{2+} cations are reduced preferentially. The highly symmetrical and stable coordination of the S_I Ni^{2+} ions therefore renders them difficult to reduce at lower temperatures. At temperatures higher than 673 K, all the sites must be energetically equal with regard to hydrogen reduction and a decrease in the number of divalent ions takes place simultaneously at all sites. NiNa–Y-22.56 (6.60 Ni^{2+}) exhibits similar reduction behavior to NiK–Y-23.52 (6.82 Ni^{2+}/UC) (Fig. 5). However, the NiK–Y sample is reduced to a greater degree at lower temperatures. This is due to the observed lower rate of migration of Ni^{2+} ions to the hexagonal prisms for the NiK–Y sample (Figs. 1 and 2), which results in a longer residence time for the Ni^{2+} ions in the accessible large cages.

(*d*) *The Role of Reduction Time*

A series of reduction against time curves for the reduction of NiNa–Y and NiK–Y are shown in Figs. 6, 7, and 8. All the curves are characterized by an initial high level of reduction followed by a slow attain-

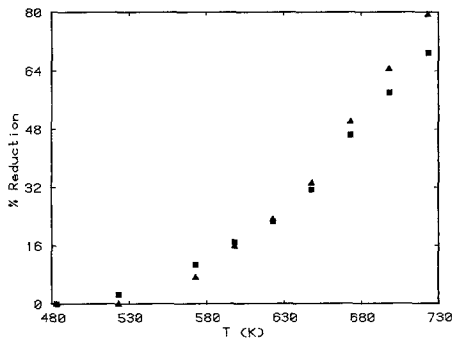

FIG. 5. Effect of reduction temperature (at a H_2 flow rate of 120 cm^3 min^{-1} for 18 h) on the degree of reduction of Ni^{2+} ions supported on NiNa–Y-22.76 (▲) and NiK–Y-23.52 (■).

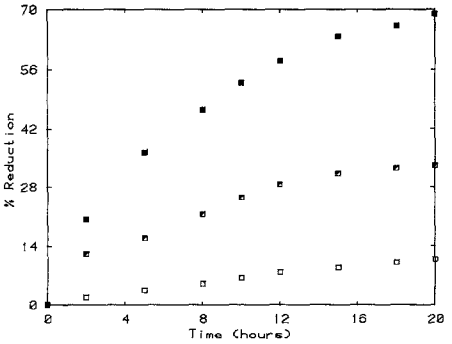

FIG. 6. Variation in degree of reduction of Ni^{2+} ions (in a 120 cm^3 min^{-1} stream of hydrogen) supported on NiK–Y-23.52 with time at 723 K (■), 648 K (◩), and 573 K (□).

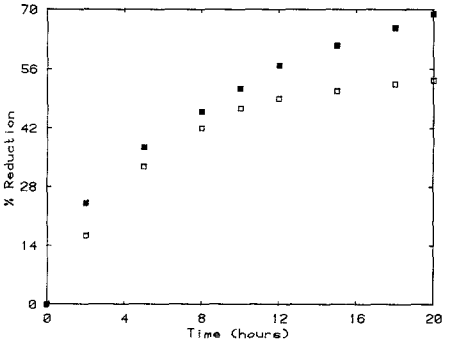

FIG. 8. Effect of reduction time on the degree of reduction (at 723 K) of Ni^{2+} ions (in a 120 cm^3 min^{-1} stream of hydrogen) supported on NiK–Y-23.52 (□) and NiK–Y-81.97 (■).

ment of the equilibrium value. This equilibrium degree of reduction is arrived at sooner at the higher reduction temperature (Fig. 6). The reduction curves for a NiNa–Y and NiK–Y sample of similar nickel loading are shown in Fig. 7. The plateau is reached at an earlier reduction time for the NiNa–Y sample at all the temperatures studied. In both cases, reduction has reached equilibrium after 18 h. This rather lengthy treatment suggests the involvement of a diffusion process, either of the hydrogen molecule into the hexagonal prisms or of the Ni^{2+} ions into the accessible large cages as proposed by Uytterhoeven *et al.* (*34*). Hydrogen molecules having a kinetic diameter of 0.24 nm should diffuse into the sodalite cages at elevated temperatures. It is therefore unreasonable to suggest that diffusion prohibition of hydrogen molecules might be the reason for the low reactivity of nickel ions situated at S_I sites. Rather, the lower reducibility of nickel ions at S_I sites must be due to the highly stable and symmetrical coordination of the structural oxygen atoms. At elevated temperatures the S_I nickel ions migrate into the supercage where they are more easily reduced. The degree of reduction data generated in this study suggest that the migration of Ni^{2+} ions from S_I sites is inhibited to a greater degree when the larger K^+ ions are present as co-cations. The values of the activation energy calculated from these curves vary considerably with the extent of reduction. The activation energy for NiK–Y-23.52 (6.82 Ni^{2+}/UC), in the temperature range 648–723 K, with 10% Ni^{2+} reduction is 33.6 kJ mol^{-1} which compares with 44.6 kJ mol^{-1} for a reduction level of 30%. The observed increase in activation energy with progressive reduction suggests that the migration of small cage Ni^{2+} ions is retarded during the reduction process.

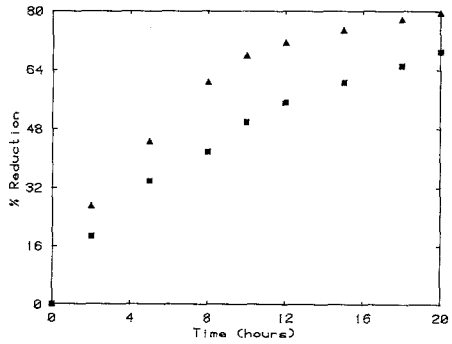

FIG. 7. Effect of reduction time on the degree of reduction (at 723 K) of Ni^{2+} ions (in a 120 cm^3 min^{-1} stream of hydrogen) supported on NiNa–Y-22.76 (▲) and NiK–Y-23.52 (■).

(*e*) *The Role of Precalcination and Heating Rates*

The effect of calcination in nitrogen at 723 K prior to reduction by hydrogen on

TABLE 3

Effect of Precalcination on Percentage Ni^{2+} Reduction

Zeolite sample	Ni^{2+}/UC	% Ni^{2+} reduction	
		Reduced at 723 K	Precalcined at 723 K
NiNa–Y-22.76	6.60	79.30	54.23
NiNa–Y-63.10	18.30	54.16	46.41
NiK–Y-23.52	6.82	68.86	40.76
NiK–Y-62.52	18.13	56.94	40.54

Ni^{2+} reducibility is demonstrated by the iodometric titration data in Table 3. The resulting levels of Ni^{2+} reduction are significantly greater for samples reduced without prior calcination. Similar observations have been made in the literature (*10–13*). The rate of temperature increase in hydrogen reduction also significantly affects the percentage of Ni^{2+} reduction as illustrated in Fig. 9. The degree of Ni^{2+} reduction is almost twice as great for the sample reduced at the lower rate of temperature increase, i.e., at a heating rate of 25 K h^{-1} compared with 1000 K h^{-1}. This again reinforces the earlier postulation that the partially dehydrated Ni^{2+} cations are reduced in the act of migrating to the S_I sites. The lower heating rates in hydrogen result in an increase in the contact time of hydrogen with the migrating, partially dehydrated nickel species and promote reduction.

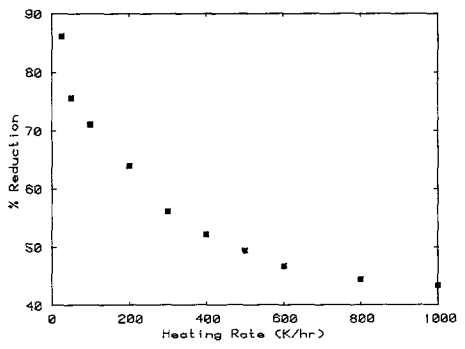

FIG. 9. Effect of the rate of heating of NiK–Y-23.52 in hydrogen (at 120 cm^3 min^{-1} for 18 h) on the level of Ni^{2+} reduction at 723 K.

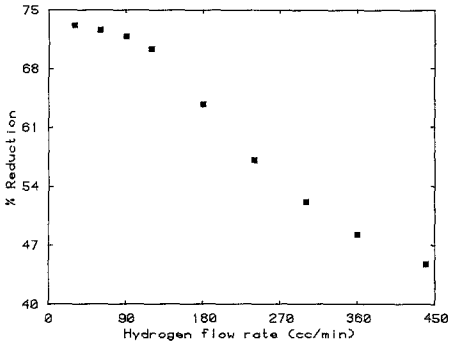

FIG. 10. Effect of hydrogen flow rate on the level of reduction of Ni^{2+} ions supported on NiK–Y-23.52 after 18 h of treatment at 723 K.

(*f*) *The Role of Hydrogen Flow Rate*

The effect of hydrogen flow rate on the reducibility of Ni^{2+} cations was also investigated, the results of which are depicted in Fig. 10 for NiK–Y-23.52 (6.82 Ni^{2+}/UC). Percentage Ni^{2+} reduction increases significantly as the hydrogen flow rate is decreased from 440 to 25 cm^3 min^{-1}. The increased extent of reduction to the metallic state (from ca. 44 to 74%) with decreasing hydrogen flow rate (from 440 to 25 cm^3 min^{-1}) very likely results from a related increased efficiency of hydrogen transfer to the divalent nickel ions due to the greater contact time. An apparent saturation effect is observed at the lower flow rates, i.e., 25 to 120 cm^3 min^{-1}. These results are in complete contrast to the data reported by Bartholomew and Farrauto (*35*) for the Ni/Al_2O_3 system where Ni^{2+} reduction increased with increasing hydrogen space velocity due to an increased effective partial pressure of hydrogen at the nickel surface resulting from an increased "mixing" of hydrogen due to turbulence.

(*g*) *The Role of NH_3 Pretreatment*

In view of the report by Minachev *et al.* (*5*) that treatment with NH_3 at elevated temperatures promotes the reduction of S_I Ni^{2+} cations due to NH_3 decomposition at high temperatures to form active hydrogen

TABLE 4

Effect of NH_3 Pretreatment on Percentage Ni^{2+} Reduction

Zeolite sample	Ni^{2+}/UC	% Ni^{2+} reduction	
		Pretreated with NH_3	Reduced without pretreatment
NiNa–Y-22.76	6.60	38.14	79.30
NiNa–Y-35.73	10.42	35.40	65.35
NiK–Y-23.52	6.82	43.44	68.86
NiK–Y-35.62	10.33	30.14	53.22

which then penetrates the hexagonal prisms and promotes reduction, an investigation of this behavior (under the same conditions as Minachev's study (*5*)) was undertaken for two nickel-exchanged samples where the entire nickel complement is known to reside in the small cages. The samples were heated in flowing NH_3 (120 cm^3 min^{-1}) to a final temperature of 723 K and the NH_3 supply was maintained at this temperature for an additional 6 h. The samples were then reduced as normal for an additional 18 h. As can be seen from Table 4, this NH_3 pretreatment actually results in an overall lowering of the level of Ni^{2+} reduction. One may speculate that when nickel ions are reduced during the NH_3 pretreatment, the charge-balancing H^+ sites could conceivably react with NH_3 to form NH_4^+ ions. The bulky NH_4^+ ions may then restrict the migration of Ni^{2+} ions to the accessible sites.

CONCLUSIONS

The degree of reduction of Ni^{2+} cations supported on Y zeolites has been shown to be strongly dependent on the pretreatment conditions. The overall influence is manifested most strongly in the cation directional effect of the heat treatment. The maximum number of Ni^{2+} (ca. 12/UC) cations accommodated in the small cages is independent of the nature of the alkali cocation and the rate of calcination. However, the saturation of small cage sites in K–Y occurs at a higher temperature. It has been found that contrary to early reports, the partially hydrated samples exhibited a minor degree of Ni^{2+} reduction which increased with increasing reduction temperature. The accessible nickel cations are preferentially reduced while the migration of Ni^{2+} ions into the supercage is retarded with progressive reduction. The overall degree of reduction is promoted by using lower heating and hydrogen flow rates and inhibited by sample precalcination, higher heating rates, and ammonia pretreatments.

REFERENCES

1. Delafosse, D., *J. Chem. Phys.* **83,** 791 (1986).
2. Jacobs, P. A., "Carboniogenic Activity of Zeolites." Elsevier Science, Amsterdam, 1977.
3. Uytterhoeven, J. B., *Acta. Phys. Chem.* **24,** 53 (1978) [English transl.].
4. Gallezot, P., *Catal. Rev. Sci. Eng.* **12,** 71 (1982).
5. Minchev, Ch., Kanazirev, V., Kosova, L., Penchev, V., Gunsser, W., and Schmidt, F., *in* "Proceedings, 5th International Zeolite Conference" (L. V. C. Rees, Ed.), p. 335. Heyden & Son, London, 1980.
6. Olivier, D., Richard, M., Bonneviot, L., and Che, M., *Stud. Surf. Sci. Catal.* **4,** 193 (1980).
7. Rabo, J. A., Angell, C. L., Kasai, P. H., and Schomaker, V., *Discuss. Faraday Soc.* **41,** 328 (1966).
8. Penchev, V., Davidova, N., Kanazirev, V., Minchev, H., and Neinska, Y., *Adv. Chem. Ser.* **121,** 461 (1973).
9. Olson, D. H., *J. Phys. Chem.* **72,** 1400 (1968).
10. Suzuki, M., Tsutsumi, K., and Takahashi, H., *Zeolites* **2,** 51 (1982); Vol. 2, 185; Vol. 2, 193.
11. Narayanan, S., *Stud. Surf. Sci. Catal.* **12,** 245 (1982).
12. Bager, K. H., Vogt, F., and Bremer, H., *ACS Symp. Ser.* **40,** 528 (1977).
13. Richardson, J. T., *J. Catal.* **21,** 122 (1971).
14. Briese-Gulban, S., Kompa, H., Schrubbers, H., and Schulz-Ekloff, G., *React. Kinet. Catal. Lett.* **20,** 7 (1982).
15. Briend-Faure, M., Guilleux, M. F., Jeanjean, J., Delafosse, D., Djega Mariadassou, G., and Bureau Tardy, M., *Acta Phys. Chem.* **24,** 99 (1978) [English Trans.].
16. Narayanan, S., *J. Sci. Ind. Res.* **44,** 319 (1985).
17. Lawson, J. D., and Rase, H. J., *Ind. Eng. Prod. Res. Dev.* **9,** 317 (1970).
18. Jacobs, P. A., Nijs, H., Verdonck, J., Derouane, E. G., Gilson, J. P., and Simoens, A. J., *Trans. Faraday Soc. 1* **5,** 1196 (1979).
19. Carru, J. C., Delafosse, D., and Briend Faure, M., *Stud. Surf. Sci. Catal.* **18,** 337 (1984).

20. Egerton, T. A., and Vickerman, J. C., *J. Chem. Soc. Faraday Trans. 1* **69,** 39 (1973).
21. Exner, D., Jaeger, N. I., Nowak, R., Schulz-Ekloff, G., and Ryder, P., *in* "Proceedings, 6th International Zeolite Conference" (Olson, D. and Bisio, A., Eds.), p. 387. Butterworths, London, 1984.
22. Schrubbers, H., Schulz-Ekloff, G., and Wildeboer, H., *Stud. Surf. Sci. Catal.* **12,** 261 (1982).
23. Jeanjean, J., Delafosse, D., and Gallezot, P., *J. Phys. Chem.* **83,** 2761 (1979).
24. Briend-Faure, M., Jeanjean, J., Kermarec, M., and Delafosse, D., *J. Chem. Soc. Faraday Trans. 1* **74,** 1538 (1978).
25. McDaniel, C. V., and Maher, P. K., *in* "Zeolite Chemistry and Catalysis," ACS Monograph, Vol. 121, p. 285 (1976).
26. Keane, M. A., *in* "A Catalytic and Characterization Study of the Effects of Alkali Metal Cations on Nickel and Other Transition Metals in Y Zeolite Catalysts," Vols. I and II. PhD thesis, N.U.I., 1988.
27. Barrer, R. M., Davies, J. A., and Rees, L. V. C., *J. Inorg. Nucl. Chem.* **31,** 2599 (1969).
28. Breck, D. W., "Zeolite Molecular Sieves: Structure, Chemistry and Use." Wiley, London, 1973.
29. Smith, J. V., *Adv. Chem. Ser.* **101,** 171 (1971).
30. Gallezot, P., and Imelik, B., *J. Phys. Chem.* **77,** 652 (1973).
31. Delafosse, D., *Stud. Surf. Sci. Catal.* **5,** 237 (1980).
32. Suzuki, M., Tsustsumi, K., and Takahashi, H., *Zeolites* **2,** 51 (1981).
33. Garbowski, E., Primet, M., and Mathieu, M. V., *in* "Proceedings, 4th International Conference on Molecular Sieves, Chicago, 1977," Paper No. 24.
34. Beyer, H., Jacobs, P. A., and Uytterhoeven, J. B., *Faraday Trans. 1* **5,** 237 (1980).
35. Bartholomew, C. H., and Farrauto, R. J., *J. Catal.* **45,** 41 (1976).